Computers and Chemical Engineering 202 (2025) 109317

Contents lists available at ScienceDirect

Computers and Chemical Engineering

journal homepage: www.elsevier.com/locate/compchemeng

Exploring the circularity of brine valorisation through neural network modelling of an electrodialysis with bipolar membranes pilot plant

Virruso G.[a], Tamburini A.[a], Cipollina A.[a,*], Bogle I. D. L.[b], Micale G. D. M.[a]

[a] Dipartimento di Ingegneria, Università degli studi di Palermo, Viale delle scienze Ed. 6, Palermo 90128, Italy
[b] Centre for Process Systems Engineering, Department of Chemical Engineering, University College London, Torrington Place, London WC1E 7JE, United Kingdom

ARTICLE INFO

Keywords:
BMED
Economic evaluation
ANN
Process configuration
Saline feed

ABSTRACT

Electrodialysis with bipolar membranes (EDBM) is an innovative electro-membrane technology capable of simultaneously producing acid and base streams. EDBM can be employed for in situ production of chemicals, reducing transportation and storage costs, or integrated with other technologies into circular approaches for the valorisation of brines, recovering high-value materials. Innovative schemes, which foresee feeding the chemicals compartment with a brine instead of water, can be adopted in those cases in which salty acid and/or alkaline solutions can be utilised. In this way, the brine treatment capacity of the process is increased and, at the same time, the water consumption is reduced. The aim of the present work is to model EDBM's behaviour when these innovative saline feed schemes are employed. Due to the challenge of describing the process with a mechanistic approach, related to the non-ideal behaviour of the membranes and the ion interactions in multi-ionic systems, a data-driven model, based on neural networks, was developed. A set of data obtained from a semi-industrial scale EDBM unit was utilised to train and validate a neural network model. The network is capable of describing the different behaviours with high accuracy. Results revealed that all the innovative schemes can become attractive depending on water cost. The Water-Salt-Salt scheme produces the lowest levelized cost of sodium hydroxide at a concentration of 0.5 mol L^{-1}, with a value of approximately 220 € ton^{-1} in favourable conditions. This suggests that in addition to environmental benefits, an economic improvement can be obtained selecting these innovative schemes.

1. Introduction

Circular economy (CE) approaches appear essential to improve the sustainability of industrial processes. The key idea is to create a cycle that minimises resource utilisation as well as the production of waste streams (Uwuigbe et al., 2025). This reduces resource depletion, costs associated with transportation and storing, the dependence on other countries as well as prevents resource dispersion in the environment. Despite the relatively simple concept of CE, researchers face many challenges in designing treatment approaches which are effective in minimising the discharged fraction and, at the same time, environmentally sustainable. This CE concept has been extensively studied in the field of seawater brines, which are mainly produced by desalination processes and saltworks (Morgante et al., 2024; Vallès et al., 2023). Indeed, several elements are abundant in seawater, apart from sodium and chloride, such as Magnesium, Calcium, Boron, Sulphates, and Carbonates, among others (Kumar et al., 2021). Brines present a higher concentration compared to seawater, which is approximately 2 times larger in seawater desalination (M. Reig et al., 2016) and up to 20–40 times larger in saltwork (Vallès et al., 2023). The larger concentration enables or facilitates the recovery of resources, which needs to be done in fractionated steps to maintain a high purity. This is typically achieved by alternating selective separation steps with concentration processes (Meng et al., 2021). Selective separation can be obtained with membrane technologies, such as nanofiltration (Morgante et al., 2024) or selectrodialysis (M. Reig et al., 2016), thermal crystallization (A. Culcasi et al., 2022), reactive precipitation (Vassallo et al., 2021) and selective adsorption (Ye et al., 2019). To adopt reactive precipitation and adsorption processes, it is necessary to supply chemical reagents, such as acid and base streams (Kumar et al., 2021). Purchasing them from the market will significantly affect the economics and, more importantly, the circularity of the CE approach. Thus, it becomes imperative to produce in situ all chemical reagents, starting from the available waste brine. ElectroDialysis with Bipolar Membranes (EDBM) perfectly matches this requirement, representing a motive gear of the CE

* Corresponding author.
E-mail address: andrea.cipollina@unipa.it (C. A.).

https://doi.org/10.1016/j.compchemeng.2025.109317
Received 31 March 2025; Received in revised form 24 July 2025; Accepted 29 July 2025
Available online 29 July 2025

Nomenclature

Symbols

$Acid_{value}$ (€ ton^{-1}) Acid value
A_m (m^2) Active membrane area
EPF_{cost} (A m^{-2}) Electrodes, plates and frames cost
E_{cost} (€ kWh^{-1}) Electricity cost
IM_{cost} (€) Installed membrane cost
$LCoNaOH$(€ $ton-1$) Levelised cost of sodium hydroxide y (y)
Generic year
$Maint_{cost}$ (€) Maintenance cost
M_{lt} (y) Membranes and spacers lifetime
$MWp\left(gmol^{-1}\right)$ Molecular weight of product p
N_p (-) Number of points
N_{tr} (-) Number of triplets
PE_{cost} (€) Peripheral equipment cost
PE_{lt} (y) Peripheral equipment and electrodes lifetime
P_{lt} (y) Project lifetime
TS_{cost} (€) Total stack cost
U_{ext} (V) External voltage
W_h (h y^{-1}) Working hours
W_{cons} (m^{3}y^{-1}) Water consumption
W_{cost} (€ m^{-3}) Water cost
tr_{cost} (€ m^{-2}) Specific triplet cost
h (-) Generic experimental variable
C (mol L^{-1}) Molar concentration
F (L min^{-1}) Volumetric flowrate
ICI (€) Initial capital investment
PC_p (ton y^{-1}) Productivity of the generic product p
TEC (€) Total energy consumption
W (-) Weight matrix
a (-) Generic predicted variable
bi (-) Bias vector
i (A m^{-2}) Current density
j (-) Discount rate

Abbreviations

AEM Anion exchange membrane
BM Bipolar membrane
CE Circular economy
CEM Cation exchange membrane
EDBM Electrodialysis with bipolar membranes
ICI Initial capital investment
LCoNaOH Levelized cost of sodium hydroxide
MSE Mean Squared error
PV Photovoltaic
SSS Salt-salt-salt scheme
SWS Salt-water-salt scheme
TEC Total energy consumption
WSS Water-salt-salt scheme
WWS Water-Water-Salt or Standard feed and bleed scheme

approaches. The brine is fed to EDBM along with demineralised water, while electrical energy is used to desalinate the brine as well as to produce an acid and a base stream. To obtain this, monopolar cation (CEM) and anion (AEM) exchange membranes are used to selectively transport ions between solutions, depending on their charge, while bipolar membranes (BM), are employed for protons and hydroxide ions generation, through water dissociation (Strathmann, 2004). The water dissociation reaction takes place in the interlayer, formed between the anion-exchange and the cation exchange layers of the BM (Strathmann et al., 1997). The three types of membranes are stacked by positioning net spacers between them, which form the solution channels. Specifically, three different solution channels are obtained: i) the salt channel between the monopolar membranes (i.e., CEM and AEM); ii) the acid channel between the AEM and the cation exchange layer of the bipolar membrane; and iii) the base channel between the CEM and the anion exchange layer of the bipolar membrane. The sequence of three membranes separated by net spacers represents the repetitive unit of an EDBM stack, which is known as triplet (Trivedi et al., 1997). Several triplets can be installed in a commercial-scale stack (up to a few hundred), and fed hydraulically in parallel through solution manifolds. At both ends of the stack, a couple of electrodes are placed which enable to establish an electrical potential difference. The conversion from an electrical to an ionic current inside the stack is obtained thanks to redox reactions (Pärnamäe et al., 2021). The ionic current is the result of cations movement towards the negatively charged electrode (i.e., the cathode) and anions to the positively charged electrode (i.e., the anode).

The EDBM process has been studied by conducting experimental campaigns (Ibáñez et al., 2013; Hwang et al., 2016) and developing process models to predict its performance (Roux-de Balmann et al., 2002; S. Koter and Warszawski, 2006). During the last years, the EDBM process scale-up has been considered by testing pilot scale stacks with a total active membrane area between 19.2 and 48 m^2 (Cassaro et al., 2023; Filingeri et al., 2025). Cassaro et al. (Cassaro et al., 2023), tested a pilot unit under three different process configurations (i.e., continuous, discontinuous and semi-continuous) at fixed base product concentration, and utilising different current densities in the range 200–500 A m^{-2}. Results revealed that the discontinuous closed-loop configuration leads to a high performance at medium-low current density, while at medium-high current densities it is convenient to move toward a continuous feed and bleed configuration, thanks also to the advantages related to the continuous production. Filingeri et al. (Filingeri et al., 2025) explored the effect of different operating pressures (i.e., in the range of 0.5–1.5 barg) between adjacent compartments in an EDBM pilot stack, operated in closed-loop mode. It was obtained that operating the EDBM unit with a higher pressure (i.e., 1.5 barg) in the acid compartment reduces the specific energy consumption to a value of 1.2 kWh kg^{-1} and to a current efficiency of 86 % at 1 mol L^{-1} base product. Virruso et al. (G. Virruso et al., 2025) compared the performance of EDBM pilot stack fed with synthetic and real seawater brines, testing two different control strategies (i.e., flowrate and pressure control). A similar performance was obtained passing from synthetic to real brine, while more pronounced improvements were observed by adopting the pressure control strategy.

Variable energy sources, such as renewable energy, were also considered to power the EDBM process, to improve the sustainability of chemicals production. Herrero-Gonzalez et al. (Herrero-Gonzalez et al., 2018) compared the performance of a laboratory-scale EDBM stack at constant current density and powered by a photovoltaic (PV) simulator. It was found that the adoption of a feedback control loop in the case of variable current sources leads to a significant reduction in the specific energy consumption of acid product. Cassaro et al. (Cassaro et al., 2024) coupled an EDBM pilot stack with a PV simulator, demonstrating that the continuous production of acid and base streams can be achieved during the day, despite the variation in solar radiation, through the adoption of appropriate control strategies.

Recently, innovative schemes to reduce water consumption were proposed by Filingeri et al. (Filingeri et al., 2024) and tested in a batch mode with laboratory-scale stacks. These schemes use a brine to feed also the chemicals compartment instead of demineralised water. As a result, chemical solutions with a salt content are obtained, which can be used in applications where a salt background can be tolerated or can even have a positive effect. As an example, in desalination plants, these chemicals are needed to perform pH correction of the inlet streams and to conduct cleaning procedures (Fernandez-Gonzalez et al., 2016), thus the salt background does not affect the processes. In reactive precipitation processes, the use of alkali or acidified brines can have a positive effect on the supersaturation level, which is responsible for the crystal size (Battaglia et al., 2024). These innovative saline feed schemes were also tested at pilot plant scale by changing the main process variables (i.e., current density and solution flowrates) in a wide range of common operating conditions (G. Virruso et al., 2025), adopting the continuous feed and bleed configuration. This configuration results the most promising to scale up the process on an industrial level (Cassaro et al., 2023). Regarding the modelling of the EDBM process, mechanistic models were mainly adopted, with lumped (Mier et al., 2008; S. Koter and Warszawski, 2006) or distributed parameters along the main flow direction (A. Culcasi et al., 2022; León et al., 2022). To comprehensively describe the EDBM process, undesired detrimental phenomena such as concentration polarisation, osmotic and electro-osmotic water fluxes, diffusive fluxes, and parasitic currents should be accounted for, leading to a significant increase in the description complexity and in the simulation time. For multi-ionic systems such as real solutions or saline feed schemes, these effects can be exacerbated due to the ion interactions, which affect several solution and membrane properties. Therefore, the possibility of using data-driven approaches was considered. Artificial neural networks, or simply neural networks, have shown promising results in modelling membrane-based processes, both in the desalination field and in wastewater treatment processes (Niemi et al., 1995; Mahadeva et al., 2018; Jawad et al., 2021). A variety of neural networks models have been proposed to predict the undesired effect of membrane fouling in processes such as microfiltration (Hamachi et al., 1999), nanofiltration (Shim et al., 2021) and reverse osmosis (Barello et al., 2014). For other membrane-based processes, such as membrane distillation, neural networks were proposed to develop *ad-hoc* control systems to effectively operate the process when powered by solar energy (Porrazzo et al., 2013). The electrodialysis process has been modelled with neural networks to predict the process performance (i.e., ions removal and separation percentage) due to variation in the operating conditions (Jing et al., 2012; Sadrzadeh et al., 2008). In the case of EDBM, it has already been proved that neural network models can predict its non-linear behaviour, also in non-stationary conditions, adopting data obtained from a mechanistic model (G. Virruso et al., 2024). Thus, neural networks appear to be an interesting alternative tool to deeply analyse EDBM operation, especially in those cases in which a much more complex phenomenological behaviour is expected as for the innovative saline feed schemes.

The aim of the present work has been to develop for the first time a neural network model, based on experimental data, to predict the behaviour of a commercial EDBM unit when operating under innovative schemes for brine valorisation and standard feed and bleed configuration. The model was also adopted to conduct an economic assessment of the innovative schemes in three different scenarios (i.e., base, island and industrial), by changing electricity and water costs, highlighting the attractiveness of these operating schemes in reducing environmental impact and costs associated with acid and base productions.

2. Method

2.1. Experimental set-up and process configurations

The experimental data employed to train the neural network model were collected with an EDBM pilot plant, which consists of a pumping station, equipped with all the instrumentations to monitor and control the unit, an EDBM stack (FT-ED1600–3, FuMA-Tech GmbH, Germany), with 40 triplets, each one with an active membrane area of 0.16 m^2, and a Direct Current (DC) power supply (AF02 GIUSSANI S.r.l.), capable of applying up to 80 V and 200 A. Detailed information about the EDBM pilot plant can be found in a previous work (Cassaro et al., 2023).

Three innovative EDBM process schemes, which represent a variation of the conventional feed and bleed configuration, were tested, along with the standard feed and bleed mode, under different operating conditions. The process schemes differ for the streams fed to the acid and base compartments. Specifically, in standard feed and bleed mode water is fed to these compartments, while in the innovative schemes a brine is used. This choice enables to improve the brine treatment capacity of EDBM as well as reducing water consumption. A schematic representation of the standard feed and bleed configuration and of the innovative process schemes is reported in Fig. 1. The standard feed and bleed configuration, indicated also Water-Water-Salt (WWS) scheme, due to the solution adopted as feed in the acid, base and salt compartments, respectively, produces high-purity acid and base streams and a brine with a reduced salt content. In the Salt-Water-Salt (SWS) scheme, demineralised water is fed to the base compartment, while a brine is pumped in the acid and salt compartments. These feed solutions allow to produce a high-purity alkaline solution, an acidified brine, and a low-concentrated salt solution. The Water-Salt-Salt (WSS) is symmetrical to the previous scheme, with the acid compartment fed with demineralised water and a brine supplied to the base and salt compartments. The outlet solutions for this scheme are an alkaline brine, a high-purity acid stream and a low-concentrated brine. In Salt-Salt-Salt (SSS) scheme all compartments are fed with a brine, thus the produced solutions are an acidified brine, an alkaline brine and a low-concentrated brine.

2.2. Data adopted for the neural network model

Experimental data used to train the neural network model were collected in four different tests, in which each of the schemes reported in Fig. 1 was tested. In each test, four operating conditions were evaluated by changing the current density and the solution flowrates as reported in Table 1.

Two different current densities (i.e., 200 and 400 A m^{-2}) were considered as representative of typical operating conditions of EDBM. The solution flowrates reported in Table 1 are the outlet flowrate from the stack and thereafter they will be indicated as flowrate for the sake of brevity. A negligible variation between inlet and outlet flowrate of the same compartment can be assumed for the feed and bleed configuration. A constant salt flowrate was set at each current density, maintaining a fixed ratio between these two variables. Acid and base flowrate were set equal to each other, and two different values were tested at fixed current density. Passing from a current density of 400 A m^{-2} to 200 A m^{-2}, the values of acid and base flowrates tested were halved, thus maintaining a perfectly proportional to the one tested at 400 A m^{-2}. The brine used to feed the salt and the chemical compartment, depending on the process scheme, was a synthetic solution of sodium chloride with a concentration of 1 mol L^{-1}, emulating reverse osmosis permeate. When the chemical compartments were fed with water, seawater reverse osmosis permeate, with a conductivity of approximately 400 μS cm^{-1}, was used. The experimental tests of these innovative schemes were published in a previous work, to which the reader is referred for further details (G. Virruso et al., 2025).

2.3. Neural network model

To develop a neural network model, it is important to define the input and output variables needed to comprehensively describe the system. To this end, several measured variables can be used, also depending on the measurement instruments available. Aiming to reduce the complexity of the model, the most significant variables were considered here. Specifically, outlet chemical concentrations and external voltage values were used as model output, while, as input, outlet flowrates, salt presence in the chemicals compartments, and current density supplied to the system were selected. The current density and the solution flowrates are the variables with a greater impact on the outputs, and they are commonly set during EDBM operation (Virruso et al., 2023). The presence of the brine in the acid and base compartments allows to select the operational process scheme (i.e., standard

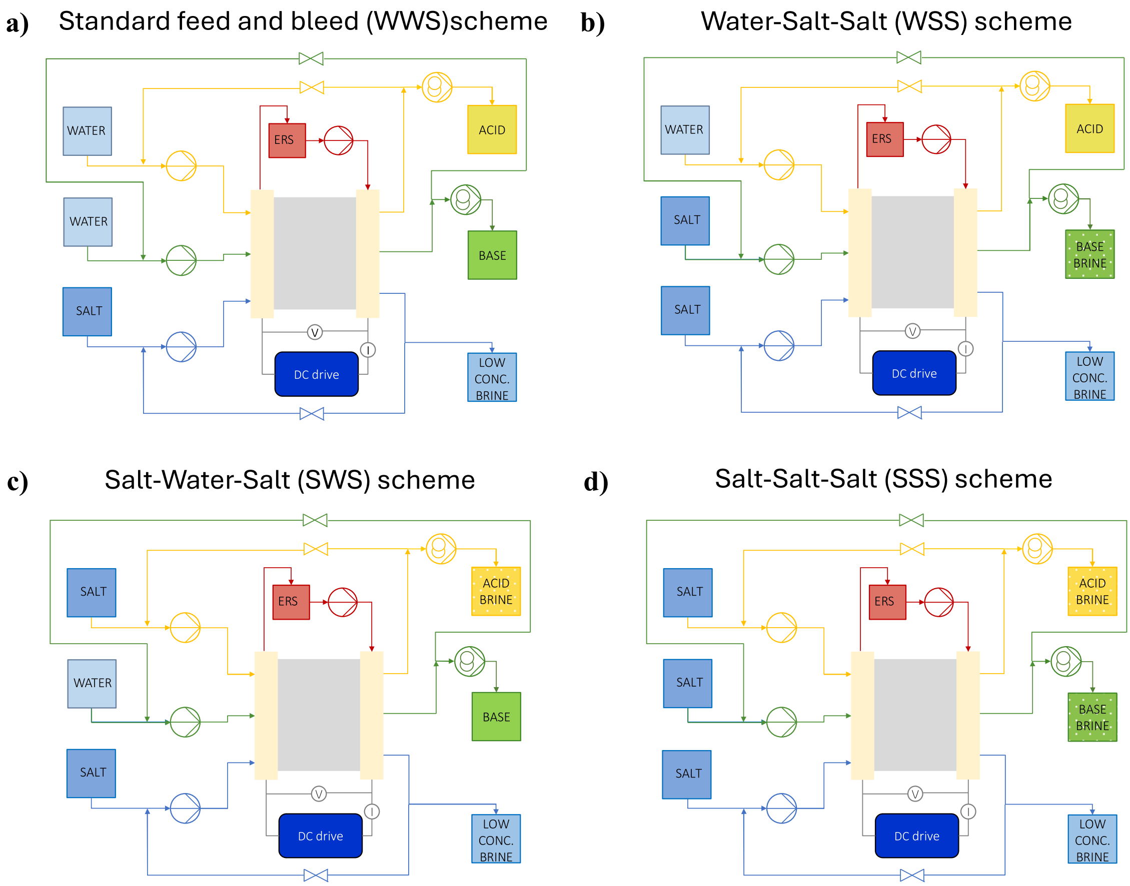

Fig. 1. Schematic representation of the feed and bleed process configuration adopting (a) conventional feed and bleed scheme (WWS), and schemes for improving brine treatment capacity and reducing water consumption: (b) Salt-Water-Salt (SWS) scheme, (c) Water-Salt-Salt (WSS) scheme, and (d) Salt-Salt-Salt (SSS) scheme.

Table 1
Operative conditions adopted for each operative scheme reported in Fig. 1.

Case	i ($A\ m^{-2}$)	F_{acid} ($L\ min^{-1}$)	F_{base} ($L\ min^{-1}$)	F_{salt} ($L\ min^{-1}$)
A	400	2	2	1.5
B	400	1	1	1.5
C	200	1	1	0.75
D	200	0.5	0.5	0.75

feed and bleed or innovative schemes). Specifically, a value of 1 is used in the case of a brine feed in acid and base compartment, while a value of 0 is used when the these compartments are fed with water.

The outputs were selected to evaluate the chemicals concentrations reached, in terms of protons and hydroxide ions, and the electrical energy consumed by the system. It is important to note that the use of the outlet flowrates allows to correctly account for the quantity of the produced chemicals as well as provides an indication of the water and energy consumptions.

A neural network with a single hidden layer was utilised, as it results sufficient in most applications (Shojai Kaveh et al., 2008; Jokić et al., 2020) and allow to reduce the number of network parameters. Sigmoid and linear transfer functions were adopted in the hidden and in the output layer, respectively. To define the number of nodes in the hidden layer, different networks were trained by changing the number of nodes between 1 and 3, to limit the number of parameters up to 33 (3 nodes in the hidden layer). To train the network, *MATLAB's fitnet function* was utilised, adopting the Bayesian Regularization training algorithm. This algorithm is recommended for small datasets because the validation set is not needed to stop the training process and it also prevents overfitting problems (Hagan et al., 2014). The data described in section 2.2 were adopted to develop the neural network model. These data were manually distributed into two sets: training and testing sets. A total of 12 data points were used for the training, while 4 data points were employed for testing the network, in a way that the testing set contains a data point for each process scheme. Several combinations of data divisions between training and testing were evaluated and the one that led to the best performance was selected. It was avoided to use other cross-validation techniques to further curtail the training dataset, which results limited in size due to the difficulties of obtaining data at pilot plant scale. As a cost function, the Mean Squared Error (MSE) was employed, defined as follows:

$$MSE = \frac{1}{N_p}\sum_{k=1}^{N_p}(a(k) - h(k))^2 \qquad (1)$$

where *a(k)* represents the *k-th* predicted value and *h(k)* is the desired value. The summation is extended to the number of points (i.e., N_p). To account for the 3 outputs an average MSE was used. Moreover, to avoid issues related to the different scales of inputs and outputs, they were rescaled in the range 0–1, dividing them by their maximum value (all the input variables have positive values). This normalisation process reduces the effect of higher relative importance due to the higher absolute value of the outputs. A random weight initialisation was utilised, with values also in the range 0–1. Further information about the neural network model can be found in the Supplementary Material (Table S1). The best performance was obtained with a network with 3 nodes in the hidden layer (i.e., corresponding to a total number of weights equal to 33), with a value of MSE ≈ 0.00028. The trend of the MSE during the training processes and the neural network model architecture are reported in Fig. 2.

The predictions of the obtained neural network model are shown in

Fig. 3 in comparison with the experimental results, for training and testing points. The three outputs are well predicted in their entire range of values, with a maximum absolute deviation between 4.1 % and 7.2 %, while, on average, deviations of approximately 2 % were obtained for all the outputs. It should be observed that the testing points are predicted with similar accuracy compared to the training points, proving that the network is capable of generalising.

2.4. Economic model

An economic model is adopted to examine the innovative schemes along with the standard feed and bleed mode in terms of the levelized cost of sodium hydroxide (LCoNaOH). The latter represents the greater value product of EDBM when a brine containing mainly sodium chloride is adopted. Capital and operating costs of the EDBM process are considered in the economic model as well as compound interest to account for the money value change over time. The economic model uses both the inputs and the outputs of the neural network model to compute the LCoNaOH and it has been implemented in Microsoft Excel®. Below the main equations of the economic model are reported.

Process variables such as acid and base productivity and water consumption are calculated through the equation reported below. The acid and base productivities, expressed in ton y^{-1}, are computed as follows:

$$PC_p = 0.48 \cdot MW_p \cdot F_p \cdot C_p \tag{2}$$

where MW_p is the molecular weight of hydrochloric acid or sodium hydroxide, F_p is the volumetric flowrate of product p and C_p is the molar concentration of product p.

The water consumption, expressed in m^3 y^{-1}, is given by the following equations, depending on the adopted process scheme:

$$WWS \rightarrow W_{cons} = (F_{acid} + F_{base}) \cdot 60 \cdot 10^{-3} \cdot W_h \tag{3}$$

$$SWS \rightarrow W_{cons} = (F_{base}) \cdot 60 \cdot 10^{-3} \cdot W_h \tag{4}$$

$$WSS \rightarrow W_{cons} = (F_{acid}) \cdot 60 \cdot 10^{-3} \cdot W_h \tag{5}$$

$$SSS \rightarrow W_{cons} = 0 \tag{6}$$

where W_h represents the working hours in a year.

The capital costs accounts for EDBM stack cost and the peripheral equipment to operate it. The installed membrane, expressed in €, is evaluated through the equation reported below:

$$IM_{cost} = tr_{cost} \cdot N_{tr} \cdot A_m \tag{7}$$

where tr_{cost} is the specific triplet cost, N_{tr} represents the installed number of triplets in the EDBM stack and $A_m$is the active membrane area.

The electrode and plates and frames cost, expressed in €, is given by:

$$EPF_{cost} = 0.5 \cdot IM_{cost} \tag{8}$$

The total stack cost, expressed in €, is computed as follows:

$$TS_{cost} = IM_{cost} + EPF_{cost} \tag{9}$$

The peripheral equipment cost, expressed in €, is evaluate through the following equation:

$$PE_{cost} = 1.2 \cdot TS_{cost} \tag{10}$$

The initial capital investment, expressed in €, is given by:

$$ICI = TS_{cost} + PE_{cost} \tag{11}$$

The operative costs considered in the economic analysis are the maintenance and total energy consumption costs. Maintenance cost, expressed in € y^{-1}, is set to 10 % of the initial capital investment (Lei et al., 2020):

$$Maint_{cost} = 0.1 \cdot ICI \tag{12}$$

The total energy consumption, expressed in € y^{-1}, is computed through the equation reported below:

$$TEC = 1.1 \cdot U_{ext} \cdot i \cdot A_m \cdot 10^{-3} \cdot W_h \cdot E_{cost} \tag{13}$$

Where U_{ext} is the external voltage applied to the stack, i is the current density, and the coefficient 1.1 accounts for the electrical consumption of the stack and peripheral equipment. The latter is considered to be 10 % of the electrical consumption of the EDBM stack

The LCoNaOH, expressed in € ton^{-1}, is calculated by adopting the following formula:

$$LCoNaOH = \frac{1}{PC_{Base}} \left(Maint_{cost} + TEC + W_{cost} \cdot W_{cons} - Acid_{value} \cdot PC_{Acid} + \frac{ICI \cdot (1+j)^{10} + IM_{cost} \cdot (1+j)^5}{\sum_{y=1}^{10} (1+j)^{(10-y)}} \right) \tag{14}$$

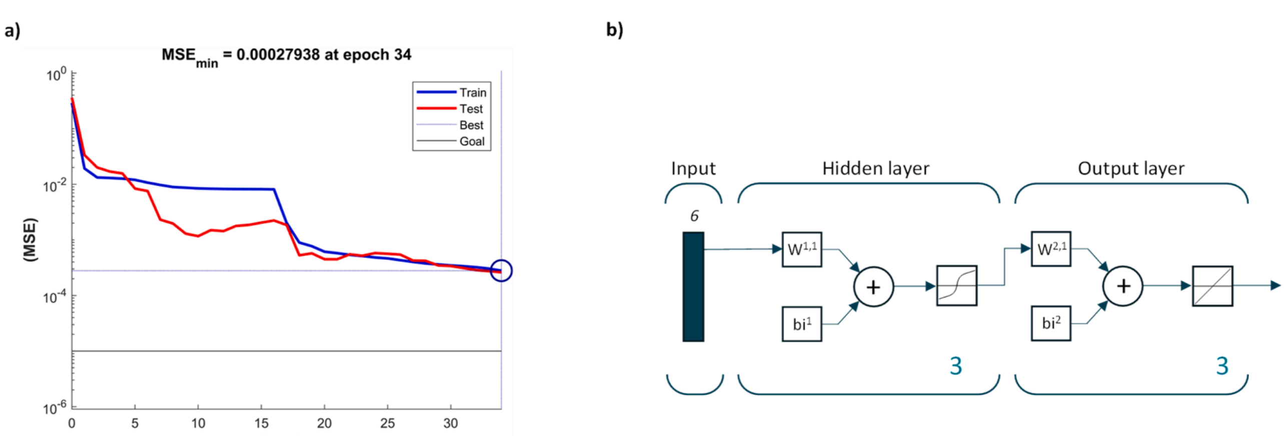

Fig. 2. a) trends of MSE of testing and training sets as a function of the number of epochs during the training phase; b) structure of the feedforward neural network used to model the EDBM process.

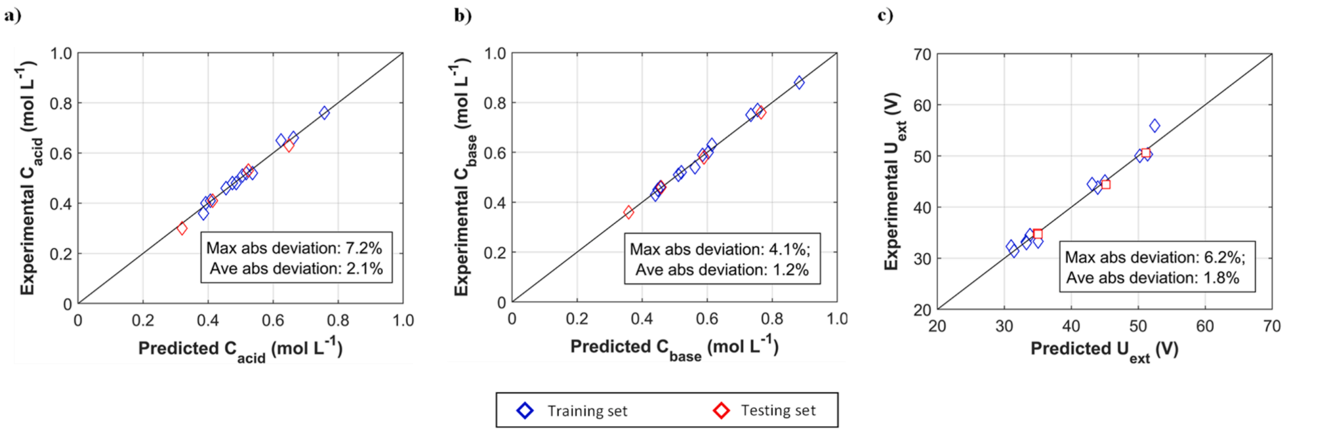

Fig. 3. Comparison between the network protections (x-axis) and experimental values (y-axis) for training and testing sets: a) concentration of the acid product in terms of protons; b) concentration of the base product in terms of hydroxide ions; c) externally applied voltage.

where W_{cost} represents the water cost, W_{cons} is the water consumption, $Acid_{value}$ is the value of the acid product, y refers to the generic yaer and j is the discount rate.

Table 2 summarises the process parameters adopted to conduct the economic analysis, while Table 3 reports the economic parameters fixed in the analysis.

Three scenarios, namely Reference, Island and Industrial, were considered to evaluate the innovative schemes. Different costs of electricity and demineralised water were assumed for each scenario to show how these cost variations can significantly affect the economic convenience of these innovative schemes. To compute the LCoNaOH it is necessary to fix a selling price for the other product (i.e., the acid), but its purity, which is related to the salt background, varies depending on the process scheme adopted. For this reason, it was decided to fix a value of 75 € ton^{-1} for the WWS and WSS schemes, in which demineralised water is fed to the acid compartment, and a value of 25 € ton^{-1} for the SWS and SSS schemes, in which a brine is used to feed the acid chamber. The scenarios are summarised in Table 4.

Table 3
Economic parameters set in the economic model.

	Value	Unit	Reference
Economic parameters/variables			
Discount rate (j)	5	%	(A. Culcasi et al., 2022)
Membrane and spacers lifetime (M_{lt})	5	y	(Lee et al., 2002)
Peripherals and electrodes lifetime (PE_{lt})	10	y	(G. Virruso et al., 2024)
Project lifetime (P_{lt})	10	y	(A. Culcasi et al., 2022)
Working hours (W_h)	8000	h y^{-1}	(A. Culcasi et al., 2022)
Electricity cost (E_{cost})	0.05–0.15	€ kWh^{-1}	
Acid product value ($Acid_{value}$)	25–75	€ ton_{HCl}^{-1}	
Water cost (W_{cost})	0.5–3	€ m^{-3}	
Specific triplet cost (tr_{cost})	550	€ m^{-2}	(G. Virruso et al., 2024)

3. Results and discussion

3.1. Simulation of the EDBM process

The obtained neural network model was used to simulate the EDBM process under the four different operating schemes. For all the schemes the same operating conditions were considered. To test the interpolation and extrapolation capacity of the neural network model, a wide range of operating conditions, inside and outside the range of the experimental data, were predicted by changing both current density and solution flowrates. The current density was extrapolated by ± 50 A m^{-2}, compared to the range of current density used in the training process (i. e., 200–400 A m^{-2}), while inside this range it was changed with steps of 50 A m^{-2}. Acid and base flowrates were extrapolated by ± 15 % compared to the value used in the experimental data, leading to a wider range. As said in section 2.2, a fixed ratio between current density and salt flowrate was maintained in the experiments and the same ratio was set for other current densities that were not investigated in the experimental campaign. The range of acid and base flowrates, corresponding to other current densities that were not investigated in the experimental campaign, was computed by linearly interpolating or extrapolating the range used in the experimental tests, increased by ± 15 %. Within their ranges, acid and base flowrates were varied with steps of 0.05 L min^{-1} at each current density. Table 5 summarises the operative conditions assessed with the neural network model.

Table 2
process parameters considered in the economic model.

Stack parameter/variables	Value	Unit
Active membrane area (A_m)	0.16	m^2
Number of triplets (N_{tr})	40	-
Current density (i)	150–450	A m^{-2}

The results of the simulations in terms of the three model outputs are shown in Fig. 4. Acid and base concentrations are shown as a function of the corresponding flowrate for the four investigated process schemes (i. e., standard feed and bleed and innovative schemes). It can be observed that the concentration versus flowrate trends are in general non-linear, especially for high current density. This non-linear effect is related to the process efficiency, known as current utilization/efficiency, which reduces at low solution flowrate due to the undesired diffusive process, exacerbated by the combined action of higher concentration reached and high residence time inside the system. At high solutions flowrate, diffusive phenomena have a lower impact due to the reduced concentrations obtained along with the smaller residence time. Moreover, it should be noted that the concentration increases as the current density rises, due to an increase of the current utilization (G. Virruso et al., 2024). This effect is related to an increase in the relative importance between migrative fluxes, which leads to the chemicals production, and diffusive processes, which reduce the chemicals concentration. A more horizontal trend is observed in the concentration profile as a function of the solution flowrate at high current density and elevated solution flowrate, which is related to the above-mentioned effect of the current efficiency. Regarding the external voltage trend, an increase is observed

Table 4
Variables changed in the scenarios to evaluate the economic effectiveness of the innovative schemes.

Scenario	Reference				Island				Industrial			
Process schema	WWS	WSS	SWS	SSS	WWS	WSS	SWS	SSS	WWS	WSS	SWS	SSS
Acid product value (€ ton^{-1})	75[a]		25		75 [a]		25		75 [a]		25	
Electricity cost (€ kWh^{-1})	0.1[b]				0.15				0.05[c]			
Water cost (€ m^{-3})	1				3[d]				0.5[e]			

[a] Average hydrochloric acid price between the three mains marked in 2020: Europe, USA and China. (INTRATEC, 2025).
[b] Average PUN index GME in Italy in2024 (PUN, 2025).
[c] Global levelised cost of electricity for utility-scale solar photovoltaic 2023 (IRENA, 2024.).
[d] Demineralised water cost in Lampedusa island, calculated with DesalData (Estimated water cost for Lampedusa island (Italy), 2025).
[e] Demineralized water cost in Italy for consumers in 2020 (INTRATEC, 2025).

Table 5
Operating condition ranges adopted in the experimental campaign and during the simulations.

Operative range used during the experimental campaign				Operative range used during the simulation			
Current density (A m^{-2})	Salt flowrate (L min^{-1})	Acid/Base flowrate lower limit (L min^{-1})	Acid/Base flowrate upper limit (L min^{-1})	Current density (A m^{-2})	Salt flowrate (L min^{-1})	Acid/Base flowrate lower limit (L min^{-1})	Acid/Base flowrate upper limit (L min^{-1})
200	0.75	0.5	1	150	0.56	0.32	0.86
400	1.5	1	2	200	0.75	0.43	1.15
				250	0.94	0.53	1.44
				300	1.13	0.64	1.73
				350	1.31	0.74	2.0
				400	1.5	0.85	2.3
				450	1.69	0.96	2.59

as the flowrate increases and as the current density rises. The first effect can be attributed to the increase of the stack resistance, due to a lower conductivity of the acid and alkaline electrolytic solutions, while the trend with the current density is related to the higher ohmic drops inside the stack.

Comparing the different schemes, it could be easily observed that the innovative schemes lead to lower concentration, compared to the standard feed and bleed mode, under the same operating conditions. This reduction was quantified in a previous work (G. Virruso et al., 2025), leading to similar values for the WSS and SWS schemes, around 15 %, and to higher value for the SSS scheme, around 30 %. However, this reduction can be counterbalanced by the several beneficial effects in terms of water saving and a comprehensive economic analysis is necessary in order to evaluate the economic feasibility of these schemes. due to the significant reduction they pose to the water consumption.

3.2. Economic analysis results

The economic analysis considers the adoption of an EDBM stack (FT-ED1600–3, FuMA-Tech GmbH, Germany, with 40 triplets and an active membrane area of 0.16 m^2) for a project lifetime of 10 years and evaluates the levelized cost of the sodium hydroxide for the different process schemes shown in Fig. 1. It should be noted that the base stream can contain a reduced or a significant (i.e., about 1 mol L^{-1}) amount of sodium chloride background. Thus, it is assumed that the product can be used for specific applications in which this background has no impact or a positive effect, as described in the introduction. The results of the economic analysis are reported separately for the investigated scenarios.

3.2.1. Reference scenario

In the reference scenario, costs equal to 0.1 € kWh^{-1} and 1 € m^{-3} were used for electricity and demineralized water, respectively. The electricity price corresponds to the average PUN index GME in 2024 (PUN, 2025), while an intermediate cost was assumed for demineralised cost between those used in other scenarios. The corresponding LCoNaOH was calculated for each process scheme as the operative conditions vary (i.e., the current density and the chemical flowrates). These trends are shown in Fig. 5 along with the concentration versus flowrate for the base product and the distribution of the main cost factors and revenues on the LCoNaOH. In standard feed and bleed mode, a trend with a minimum is observed for all the investigated current densities. This trend is attributed mainly to the energy consumption and to the water consumption, which have a competitive effect. The energy consumption is mainly affecting the LCoNaOH at low flowrates due to the low current utilisation, while the water consumption has a major effect on the LCoNaOH at high flowrate. The reduction of the LCoNaOH as the current density rises can be attributed to the current utilisation of the process, which improves due to an increase in the relative importance of migration compared to diffusive effects. In Fig. 5 the minimum LCoNaOH points are marked with a coloured circle and their bounds are delimited with horizontal grey lines, whose values are depicted in the graphs. For the innovative process schemes, the LCoNaOH presents a decreasing trend with the base flowrate, which can be attributed to the reduction of the water consumption, which is halved for the WSS and SWS schemes, compared to the WWS scheme, and absent in the SSS scheme. The WWS scheme and WSS scheme show the lowest LCoNaOH value (i.e., 380 € ton^{-1}), while a stricter range of minimum LCoNaOH points is observed for the former. The others two innovative schemes result less competitive with the WWS scheme in this scenario. Indeed, the SWS and SSS schemes have a lower bound of minimums LCoNaOH of 18.7 % and 7.5 %, respectively, higher than the corresponding value for the WWS scheme. The trends of the LCoNaOH as function of the flowrate correspond to different base concentration values, which are also reported as a function of the base flowrate in Fig. 5 for each scheme. The minimum LCoNaOH points are depicted in the corresponding concentrate versus flowrate charts, with the same coloured circles, and their range of concentrations is delimited with two horizontal grey lines. It is evident that there is a reduction of the base concentration by passing from the standard scheme to the innovative ones. Thus, it is important to use similar concentration values to effectively compare the schemes. The black triangle in Fig. 5 represents the minimum LCoNaOH obtained at a base concentration of 0.5 mol L^{-1} for each scheme. This concentration value is common to all the configurations, and it could used in the desalination and brine valorisation fields. For the black triangle points,

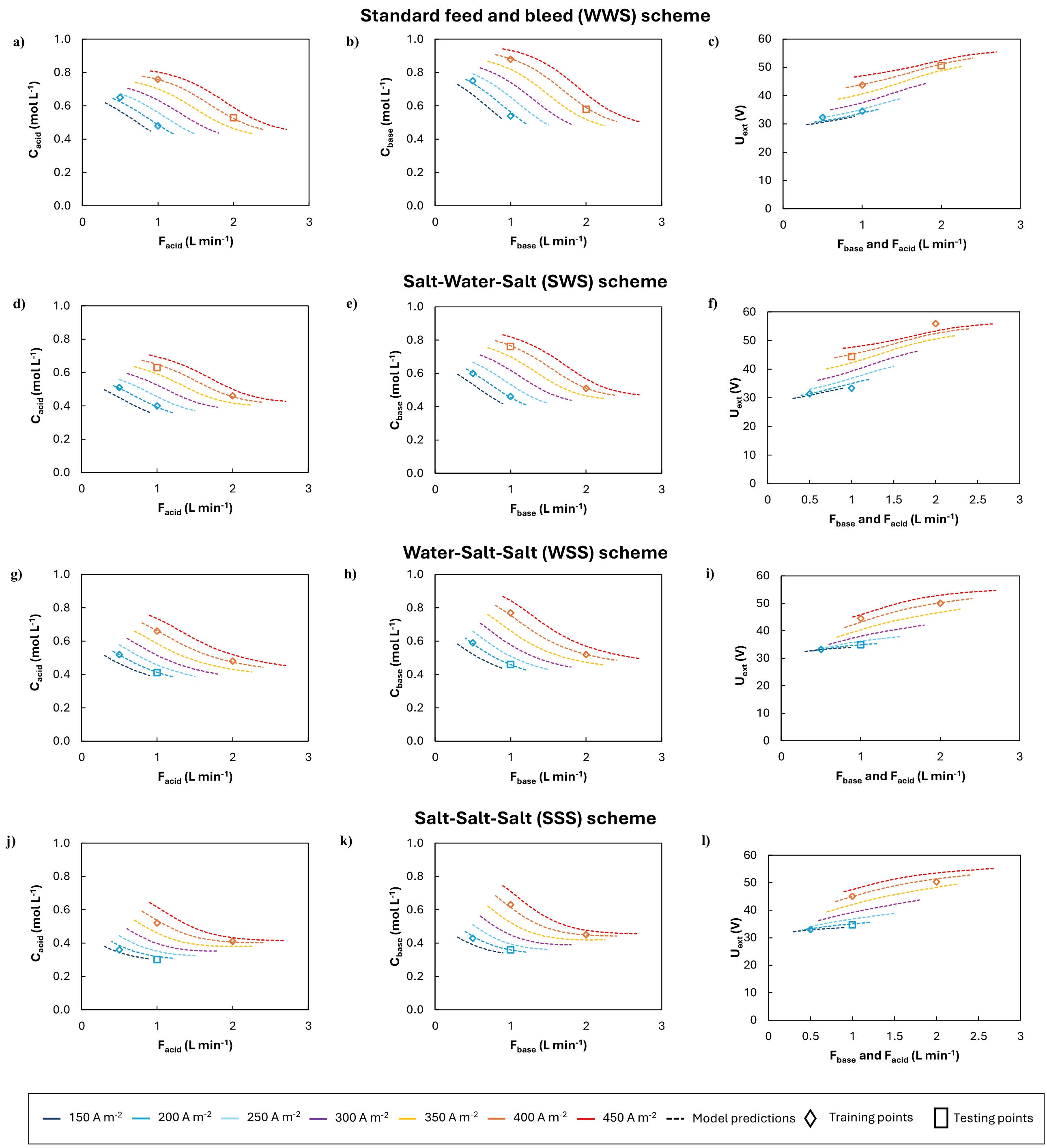

Fig. 4. Predictions of the neural network model in terms of protons concentration in the acid product, hydroxide ions concentration in the base product and external applied voltage as function of the solution flowrates. The results are shown for the four investigated process schemes (i.e., standard feed and bleed configuration and innovative schemes). Training and testing points adopted to develop and validate the model are depicted with rhombus and squares, respectively. The x-axis denoted with "F_{base} and F $_{acid}$ (L min^{-1})" refers to the fact that the two chemical flowrates were maintained equal to each other.

an analysis on the cost factors and revenue distribution in the LCoNaOH is conducted and reported in the cake charts for each scheme. The contribution of the acid product sale reduces the LCoNaOH, while all the other cost factors increase the LCoNaOH. For this reason, it was decided to represent the LCoNaOH composition with two different cake charts where all the expenditure as well as the overall expenditure and the revenue are reported. It can be observed that the lowest LCoNaOH is obtained for the WSS scheme, equal to 380 € ton^{-1}, followed by the WWS, SWS and SSS schemes, with values of 425, 478 and 554 € ton^{-1}, respectively. This inversion of the economic convenience between WSS and standard feed and bleed is related to the reduction in water consumption, which significantly affects the feed and bleed configuration at low concentrations.

3.2.2. Island scenario

The island scenario considers higher costs for electricity and demineralized water of equal to 0.15 € kWh^{-1} and 3 € m^{-3}, respectively. The electricity cost is assumed to be 50 % higher compared to the Reference scenario, due to the production in smaller power plants, while the demineralised water cost was estimated by simulating the seawater

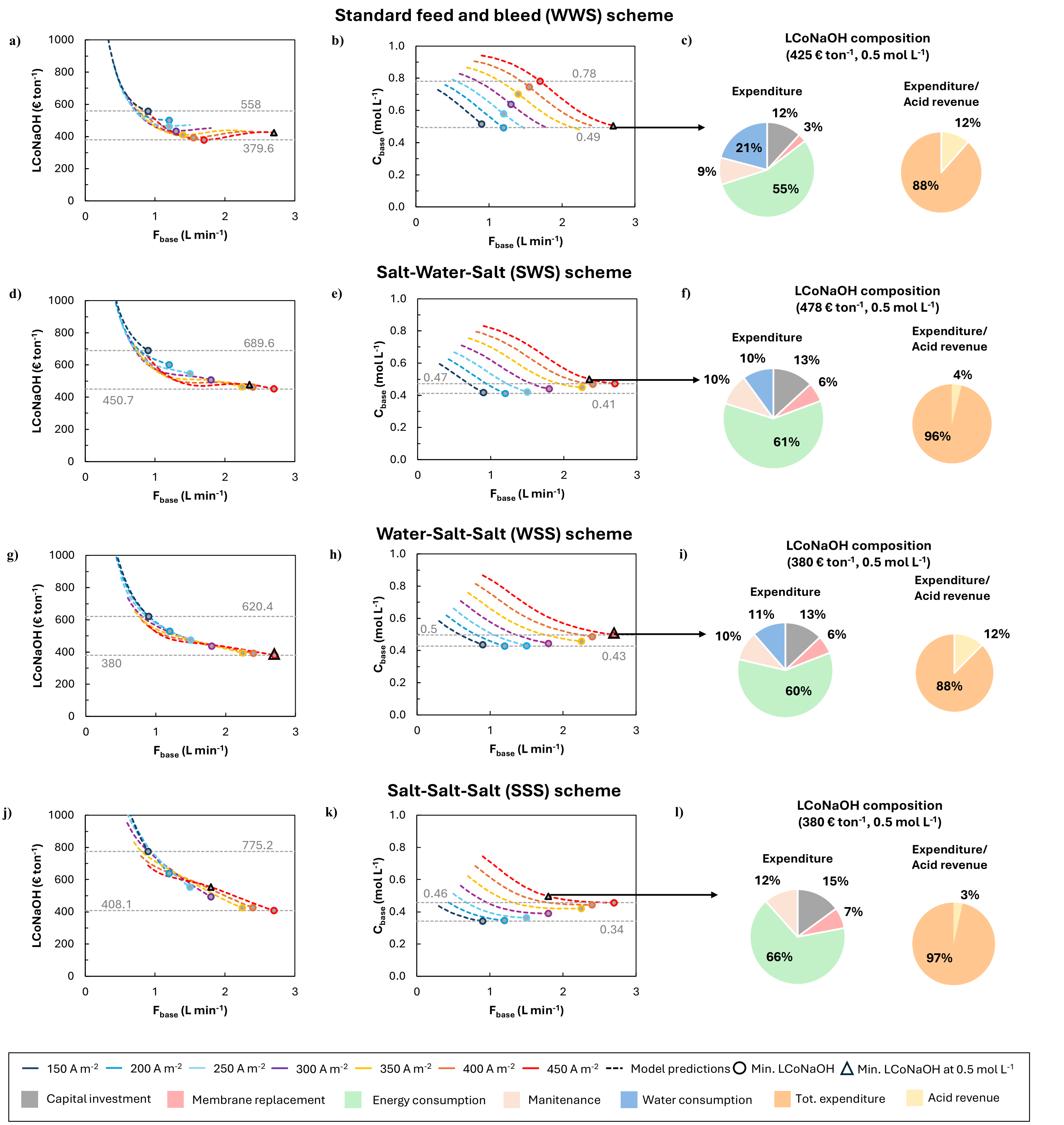

Fig. 5. Trends of the levelized cost of sodium hydroxide (LCoNaOH) as a function of the base flowrate for different current densities; concentration versus flowrate for the base product at various current densities; composition of the LCoNaOH in terms of all expenditures as well as distribution between the overall expenditure and revenue for the points marched with the black triangle (i.e., minimum LCoNaOH for a base product concentration of 0.5 mol L^{-1}). The coloured circles represent the minimum LCoNaOH for the corresponding current density. These results are shown for the different process schemes investigated in this work for the Reference scenario.

reverse osmosis plants located in Lampedusa (Italy) with Desaldata (Estimated water cost for Lampedusa island (Italy), 2025). The LCoNaOH is negatively affected by increased costs, with values higher than 550 € ton^{-1} (Fig. 6). The LCoNaOH trends are slightly different, with a major concavity in the case of the standard feed and bleed mode. This effect can be related to the higher weight at high concentration (i.e., low flowrates) of the energy consumption and at low concentration (i.e., high flowrates) of water consumption. The minimum LCoNaOH obtained in standard feed and bleed mode is 627.9 € ton^{-1} at a concentration of approximately 0.8 mol L^{-1}. For the SWS scheme, a decreasing trend of the LCoNaOH is observed at low base flowrate while at high flowrates the trends lead to almost constant values. This different behaviour at high solution flowrate can be related to the reduction of water consumption, while the acid product has a minor impact at high flowrates due to the lower value per kilogram (i.e., 25 € kg^{-1}). The WSS and SSS schemes show a decreasing trend of the LCoNaOH as function of the base flowrate. The decreasing trend is more pronounced for the SSS scheme due to absence of water consumption. Thus, reducing the

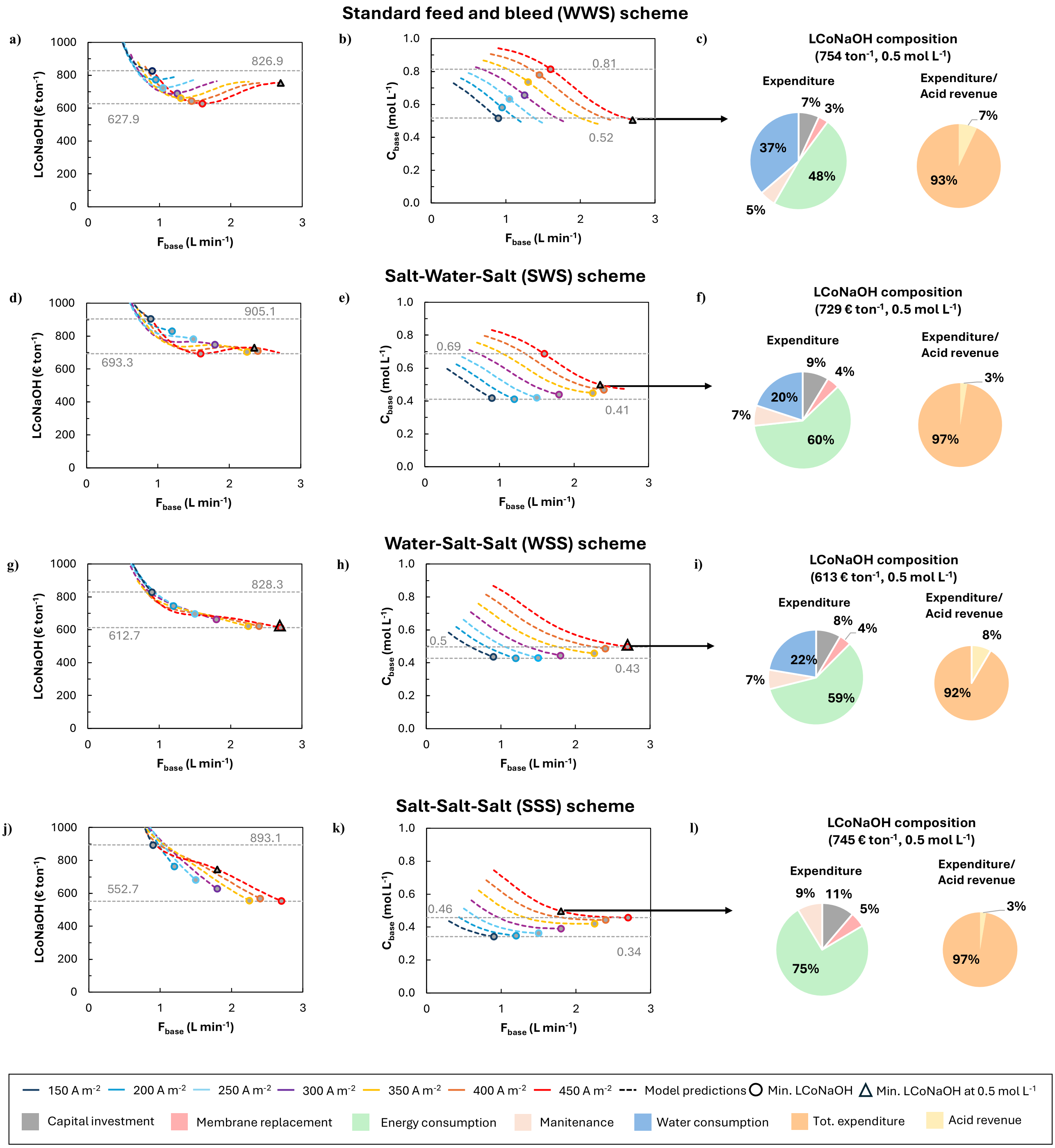

Fig. 6. Trends of the levelized cost of sodium hydroxide (LCoNaOH) as a function of the base flowrate for different current densities; concentration versus flowrate for the base product at various current densities; composition of the LCoNaOH in terms of all expenditures as well as distribution between the overall expenditure and revenue for the points marched with the black triangle (i.e., minimum LCoNaOH for a base product concentration of 0.5 mol L^{-1}). The coloured circles represent the minimum LCoNaOH for the corresponding current density. These results are shown for the different process schemes investigated in this work for the Island scenario.

concentration leads to an increase of the process performance and, consequently, a reduction of the LCoNaOH. Considering the minimum points of the LCoNaOH, the lowest value is obtained for the SSS configuration, suggesting that the water cost has a high impact on it at the selected water cost. The WSS and the standard feed and bleed schemes show similar ranges of the minimum LCoNaOH points, with a lower bound mildly lower in the case of the WSS scheme (i.e., 613 € ton^{-1}). On the other hand, the SWS shows the highest range of minimum LCoNaOH points, with values between 690–905 € ton^{-1}. Concentration versus flowrate curves are the same for all the scenarios, what changes is the position of the coloured circles, corresponding to the minimum LCoNaOH points. In terms of concentration ranges of the minimum LCoNaOH points, they vary just for the WWS and for the SWS schemes, with larger ranges compared to the Reference scenario. Comparing the process schemes at a fixed concentration of NaOH of 0.5 mol L^{-1}, it can be observed that all the innovative schemes lead to lower LCoNaOH values compared to the WWS scheme, with values between 613€ ton^{-1} and 745 € ton^{-1}, while the standard feed and bleed scheme produces a LCoNaOH of 754 € ton^{-1}. Also in this case, the lowest cost is obtained for the WSS schemes, which enables to halve the water consumption, while maintaining an acid product with a higher specific value due to the reduced salt background.

3.2.3. Industrial scenario

The industrial scenario refers to reduced electricity and demineralized water costs, of 0.05 € kWh^{-1} and 0.5 € m^{-3}, respectively. The electricity cost is compatible with a domestic production of electricity through of renewable sources (IRENA, 2024.), while the demineralized water cost represent that paid in Italy by large consumers (INTRATEC, 2025). Results, in terms of LCoNaOH, are promising with minimum LCoNaOH points in the range 220–380 € ton^{-1} for the four schemes (Fig. 7). The WWS scheme leads to trends of the LCoNaOH versus the base flowrate which decrease in the first part and reach an almost constant value for high flowrates. The other schemes show decreasing trends, which are more pronounced at high flowrate for the SSS scheme, followed by the WSS and SWS schemes. The lowest LCoNaOH was reached in the WSS scheme (i.e., 223 € ton^{-1}), which results slightly lower compared to the minimum value reached in WWS scheme, equal

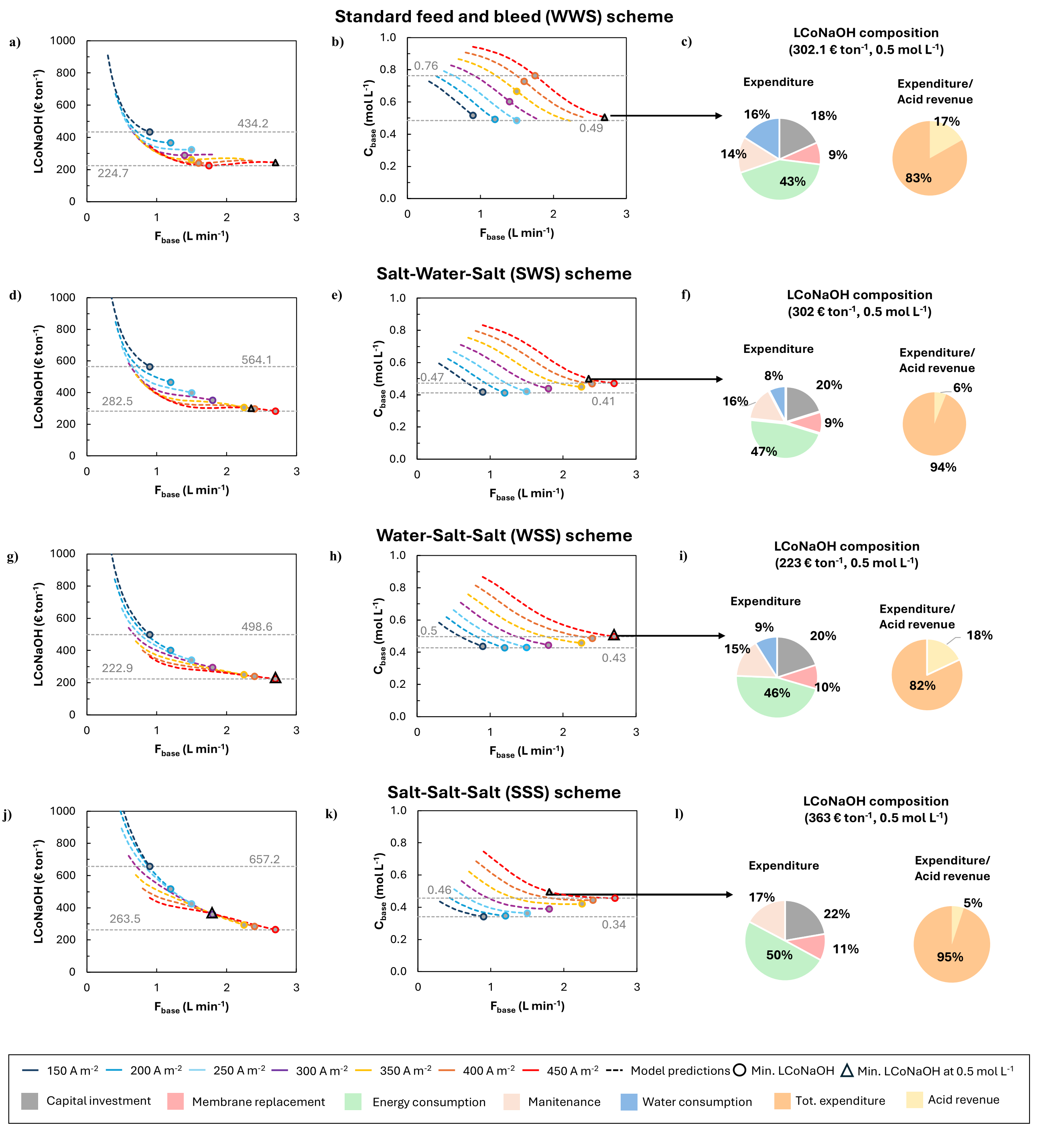

Fig. 7. Trends of the levelized cost of sodium hydroxide (LCoNaOH) as a function of the base flowrate for different current densities; concentration versus flowrate for the base product at various current densities; composition of the LCoNaOH in terms of all the expenditures as well as distribution between the overall expenditure and revenue for the points marched with the black triangle (i.e., minimum LCoNaOH for a base product concentration of 0.5 mol L^{-1}). The coloured circles represent the minimum LCoNaOH for the corresponding current density. These results are shown for the different process schemes investigated in this work for the Industrial scenario.

to 224.7 € ton^{-1}. At low current densities, the WWS scheme leads to a lower LCoNaOH compared to the WSS scheme, with a value of about 430 € ton^{-1} at 150 A m^{-2}. The other innovative process schemes produce minimum LCoNaOH values of 263.5 and 282.5 € ton^{-1} for the SSS and SWS scheme, respectively. The concentration range of the minimum LCoNaOH points results unchanged for the innovative schemes compared to the reference scenario, while for the WWS a slightly stricter range is observed, with an upper bound of the range equal to 0.76 mol L^{-1}. Looking at the LCoNaOH for target concentration of 0.5 mol L^{-1}, the lowest value of LCoNaOH was obtained for the WSS scheme, equal to 223 € ton^{-1}, followed by the WWS scheme, with a value of 245 € ton^{-1}. Also in this case, water consumption reduction brings an economic benefit, despite the reduced cost of water. The other process schemes produce LCoNaOH values of 302 and 363 € ton^{-1} for SWS and SSS schemes, respectively. Comparing the WSS and SWS schemes, the main difference in the cost factors that affect the LCoNaOH is the income of the acid product, which differs due to the salt background, leading to an income of about 3.5 times larger in the WSS scheme.

4. Conclusions and future outlooks

The present work used a neural network based modelling approach to describe the standard and the innovative feed and bleed schemes for increasing the brine treatment capacity and reducing the water consumption. The adoption of this innovative modelling approach was justified by the increased complexity of process due to the presence of sodium chloride ions also in the acid and base chambers, which affect the behaviour of the system. The neural network model was developed with a reduced number of experimental data obtained with a large-scale EDBM pilot plant, proving that neural network models can be obtained with a reduced effort if the experimental tests are well designed. The model was compared with the experimental data showing high prediction capability, with a maximum deviation of 7 % for both training and testing data, despite the quite simple structure of the network. The model was used to simulate the four process schemes under a wide range of operative conditions, testing both its interpolation and extrapolation capacity. The results of the simulation were used to conduct an economic evaluation of the schemes in three different scenarios, which differ for the electricity and water costs. The results highlight that the innovative schemes can be competitive with the standard feed and bleed configuration in various scenarios. Indeed, the reduction of water consumption is able to compensate for the reduction in the current utilisation due to the salt presence. Between the innovative schemes, the WSS scheme results the most attractive, leading to lower LCoNaOH values at 0.5 mol L^{-1} of base for all the investigated scenarios. This result can be explained by the reduction of the water consumption, while maintaining an acid product with a higher value. The SWS and the SSS schemes lead to a lower LCoNaOH compared to standard feed and bleed mode in the Island scenario, where the water cost is significantly higher. However, their LCoNaOH resulted still high compared to the WSS scheme, due to the lower acid purity and the performance reduction in the SSS scheme, related to the salt presence in both chemical compartments. These results suggest that innovative schemes can decrease the cost of producing chemical reagents up to 19 %, if a base concentration of about 0.5 mol L^{-1} is needed. The WSS produces the lower LCoNaOH value and it should be used in all the cases in which an alkaline brine can be tolerated. An extended analysis was conducted for the entire range of electricity and water costs adopted in the three scenarios analysis and reported in the Supplementary Material (Figure S1). The results confirm that all the innovative schemes can become economically preferable depending on the utility costs and break-even point are quantitatively reported. These innovative schemes improve the sustainability of industrial processes, reducing water consumption and improving the brine treatment capacity of the process, perfectly fitting the principles of circular economy approaches. Future research will focus on evaluating other process schemes and stack configurations which allow to use a saline feed of the chemicals compartment and to reduce the energy consumption of the process.

CRediT authorship contribution statement

Virruso G.: Writing – original draft, Visualization, Validation, Software, Methodology, Formal analysis, Data curation, Conceptualization. **Tamburini A.:** Conceptualization, Methodology, Supervision, Writing – review & editing, Project administration, Methodology, Funding acquisition. **Cipollina A.:** Conceptualization, Methodology, Supervision, Writing – review & editing, Project administration, Methodology, Funding acquisition. **Bogle I. D. L.:** Conceptualization, Methodology, Supervision, Writing – review & editing, Project administration, Methodology, Funding acquisition. **Micale G. D. M.:** Conceptualization, Methodology, Supervision, Writing – review & editing, Project administration, Methodology, Funding acquisition.

Declaration of competing interest

The authors declare that they have no known competing financial interests or personal relationships that could have appeared to influence the work reported in this paper.

Acknowledgments

This project has received funding from the European Union's LIFE 2021–2027 programme under Grant Agreement 101147407-LIFE23-ENV-IT-MAREMAG LIFE.

Supplementary materials

Supplementary material associated with this article can be found, in the online version, at doi:10.1016/j.compchemeng.2025.109317.

Data availability

Data will be made available on request.

References

Barello, M., Manca, D., Patel, R., Mujtaba, I.M., 2014. Neural network based correlation for estimating water permeability constant in RO desalination process under fouling. Desalination 345, 101–111. https://doi.org/10.1016/j.desal.2014.04.016.

Battaglia, G., Ventimiglia, L., Vicari, F., Tamburini, A., Cipollina, A., Micale, G., 2024. Characterization of Mg(OH)<inf>2</inf>powders produced from real saltworks bitterns at a pilot scale. Powder. Technol. 443. https://doi.org/10.1016/j.powtec.2024.119918.

Cassaro, C., Virruso, G., Culcasi, A., Cipollina, A., Tamburini, A., Micale, G., 2023. Electrodialysis with bipolar membranes for the sustainable production of chemicals from seawater brines at pilot plant scale. ACS. Sustain. Chem. Eng. 11, 2989–3000. https://doi.org/10.1021/acssuschemeng.2c06636.

C. Cassaro, G. Virruso, A. Cipollina, A. Fagiolini, A. Tamburini, G. Micale, Coupling electrodialysis with bipolar membranes with renewable energies through advanced control strategies, 2024. https://doi.org/10.1016/B978-0-443-28824-1.50330-6.

Culcasi, A., Ktori, R., Pellegrino, A., Rodriguez-Pascual, M., van Loosdrecht, M.C.M., Tamburini, A., Cipollina, A., Xevgenos, D., Micale, G., 2022a. Towards sustainable production of minerals and chemicals through seawater brine treatment using eutectic freeze crystallization and electrodialysis with bipolar membranes. J. Clean. Prod. 368. https://doi.org/10.1016/j.jclepro.2022.133143.

Culcasi, A., Gurreri, L., Cipollina, A., Tamburini, A., Micale, G., 2022b. A comprehensive multi-scale model for bipolar membrane electrodialysis (BMED). Chem. Eng. J. 437, 135317. https://doi.org/10.1016/J.CEJ.2022.135317.

Estimated water cost for Lampedusa island (Italy), 2025. https://www.desaldata.com/ (accessed July 15, 2025).

Fernandez-Gonzalez, C., Dominguez-Ramos, A., Ibañez, R., Irabien, A., 2016. Electrodialysis with bipolar membranes for valorization of brines. Sep. Purif. Rev. 45, 275–287. https://doi.org/10.1080/15422119.2015.1128951.

Filingeri, A., Herrero-Gonzalez, M., O'Sullivan, J., Rodriguez, J.L., Culcasi, A., Tamburini, A., Cipollina, A., Ibañez, R., Ferrari, M.C., Cortina, J.L., Micale, G., 2024. Acid/base production via bipolar membrane electrodialysis: brine feed streams to reduce fresh water consumption. Ind. Eng. Chem. Res. 63, 3198–3210. https://doi.org/10.1021/acs.iecr.3c03553.

Filingeri, A., Culcasi, A., Nanfara, M., Cassaro, C., Tamburini, A., Micale, G., Cipollina, A., 2025. Exploring differential pressure-induced hydraulic flows in pilot-

scale electrodialysis with Bipolar membranes. J Env. Manage 373, 123538. https://doi.org/10.1016/J.JENVMAN.2024.123538.
Hagan, M.T., Demuth, H.B., Beale, M.H., De Jesús, O., 2014. Neural Network Design, 2nd Edition.
Hamachi, M., Cabassud, M., Davin, A., Peuchot, M.Mietton, 1999. Dynamic modelling of crossflow microfiltration of bentonite suspension using recurrent neural networks. Chem. Eng. Process.: Process Intensif. 38, 203–210. https://doi.org/10.1016/S0255-2701(99)00004-5.
Herrero-Gonzalez, M., Diaz-Guridi, P., Dominguez-Ramos, A., Ibañez, R., Irabien, A., 2018. Photovoltaic solar electrodialysis with bipolar membranes. Desalination 433, 155–163. https://doi.org/10.1016/j.desal.2018.01.015.
Hwang, C.W., Jeong, M.H., Kim, Y.J., Son, W.K., Kang, K.S., Lee, C.S., Hwang, T.S., 2016. Process design for lithium recovery using bipolar membrane electrodialysis system. Sep. Purif. Technol. 166, 34–40. https://doi.org/10.1016/j.seppur.2016.03.013.
Ibáñez, R., Pérez-González, A., Gómez, P., Urtiaga, A.M., Ortiz, I., 2013. Acid and base recovery from softened reverse osmosis (RO) brines. Experimental assessment using model concentrates. Desalination 309, 165–170. https://doi.org/10.1016/j.desal.2012.10.006.
INTRATEC, Hydrochloric acid prices, historical and current, 2025. https://www.intratec.us/chemical-markets/hydrochloric-acid-price (accessed March 12, 2025).
INTRATEC, Industrial Utilities Prices & Costs | Italy, (n.d.). https://www.intratec.us/products/industry-economics-worldwide/utility/demineralized-water-italy (accessed March 12, 2025).
IRENA, Renewable power generation costs in 2023, 2024.
Jawad, J., Hawari, A.H., Zaidi, S.Javaid, 2021. Artificial neural network modeling of wastewater treatment and desalination using membrane processes: a review. Chem. Eng. J. 419. https://doi.org/10.1016/j.cej.2021.129540.
Jing, G., Du, W., Guo, Y., 2012. Studies on prediction of separation percent in electrodialysis process via BP neural networks and improved BP algorithms. Desalination 291, 78–93. https://doi.org/10.1016/j.desal.2012.02.002.
Jokić, A., Pajčin, I., Grahovac, J., Lukić, N., Ikonić, B., Nikolić, N., Vlajkov, V., 2020. Dynamic modeling using artificial neural network of bacillus velezensis broth cross-flow microfiltration enhanced by air-sparging and turbulence promoter. Membr. (Basel) 10, 1–14. https://doi.org/10.3390/membranes10120372.
Koter, S., Warszawski, A., 2006.. A new model for characterization of bipolar membrane electrodialysis of brine. Desalination. 198, 111–123. https://doi.org/10.1016/j.desal.2006.09.016.
Koter, S., Warszawski, A., 2006b. A new model for characterization of bipolar membrane electrodialysis of brine. Desalination 198, 111–123. https://doi.org/10.1016/j.desal.2006.09.016.
Kumar, A., Naidu, G., Fukuda, H., Du, F., Vigneswaran, S., Drioli, E., Lienhard, J.H., 2021. Metals recovery from seawater desalination brines: technologies, opportunities, and challenges. ACS. Sustain. Chem. Eng. 9, 7704–7712. https://doi.org/10.1021/acssuschemeng.1c00785.
León, T., López, J., Torres, R., Grau, J., Jofre, L., Cortina, J.-L., 2022. Describing ion transport and water splitting in an electrodialysis stack with bipolar membranes by a 2-D model: experimental validation. J. Memb. Sci. 660. https://doi.org/10.1016/j.memsci.2022.120835.
Lee, H.-J., Sarfert, F., Strathmann, H., Moon, S.-H., 2002. Designing of an electrodialysis desalination plant. Desalination 142, 267–286. https://doi.org/10.1016/S0011-9164(02)00208-4.
Lei, C., Li, Z., Gao, Q., Fu, R., Wang, W., Li, Q., Liu, Z., 2020. Comparative study on the production of gluconic acid by electrodialysis and bipolar membrane electrodialysis: effects of cell configurations. J. Memb. Sci. 608, 118192. https://doi.org/10.1016/J.MEMSCI.2020.118192.
Mahadeva, R., Manik, G., Verma, O.P., Sinha, S., 2018. Modelling and simulation of desalination process using artificianeural network: a review. Desalin. Water Treat 122, 351–364. https://doi.org/10.5004/dwt.2018.23106.
Meng, F., McNeice, J., Zadeh, S.S., Ghahreman, A., 2021. Review of lithium production and recovery from minerals, brines, and lithium-ion batteries. Miner. Process. Extr. Metall. Rev. 42, 123–141. https://doi.org/10.1080/08827508.2019.1668387.
Mier, M.P., Ibañez, R., Ortiz, I., 2008. Influence of ion concentration on the kinetics of electrodialysis with bipolar membranes. Sep. Purif. Technol. 59, 197–205. https://doi.org/10.1016/j.seppur.2007.06.015.
Morgante, C., Vassallo, F., Cassaro, C., Virruso, G., Diamantidou, D., Van Linden, N., Trezzi, A., Xenogianni, C., Ktori, R., Rodriguez, M., Micale, G., Xevgenos, D., 2024. Pioneering minimum liquid discharge desalination: a pilot study in Lampedusa Island. Desalination. 581. https://doi.org/10.1016/j.desal.2024.117562.
Niemi, H., Bulsari, A., Palosaari, S., 1995. Simulation of membrane separation by neural networks. J. Memb. Sci. 102, 185–191. https://doi.org/10.1016/0376-7388(94)00314-O.
Pärnamäe, R., Mareev, S., Nikonenko, V., Melnikov, S., Sheldeshov, N., Zabolotskii, V., Hamelers, H.V.M., Tedesco, M., 2021. Bipolar membranes: a review on principles, latest developments, and applications. J. Memb. Sci. 617. https://doi.org/10.1016/j.memsci.2020.118538.
Porrazzo, R., Cipollina, A., Galluzzo, M., Micale, G., 2013. A neural network-based optimizing control system for a seawater-desalination solar-powered membrane distillation unit. Comput. Chem. Eng. 54, 79–96. https://doi.org/10.1016/j.compchemeng.2013.03.015.
PUN INDEX GME, 2025. https://gme.mercatoelettrico.org/it-it/Home/Esiti/Elettricita/MGP/Esiti/PUN (accessed July 15, 2025).
Reig, M., Casas, S., Gibert, O., Valderrama, C., Cortina, J.L., 2016a. Integration of nanofiltration and bipolar electrodialysis for valorization of seawater desalination brines: production of drinking and waste water treatment chemicals. Desalination. 382, 13–20. https://doi.org/10.1016/j.desal.2015.12.013.
Reig, M., Valderrama, C., Gibert, O., Cortina, J.L., 2016b. Selectrodialysis and bipolar membrane electrodialysis combination for industrial process brines treatment: monovalent-divalent ions separation and acid and base production. Desalination. 399, 88–95. https://doi.org/10.1016/j.desal.2016.08.010.
Roux-de Balmann, H., Bailly, M., Lutin, F., Aimar, P., 2002. Modelling of the conversion of weak organic acids by bipolar membrane electrodialysis. Desalination 149, 399–404. https://doi.org/10.1016/S0011-9164(02)00863-9.
Sadrzadeh, M., Mohammadi, T., Ivakpour, J., Kasiri, N., 2008. Separation of lead ions from wastewater using electrodialysis: comparing mathematical and neural network modeling. Chem. Eng. J. 144, 431–441. https://doi.org/10.1016/j.cej.2008.02.023.
Shim, J., Park, S., Cho, K.H., 2021. Deep learning model for simulating influence of natural organic matter in nanofiltration. Water. Res. 197. https://doi.org/10.1016/j.watres.2021.117070.
Shojai Kaveh, N., Ashrafizadeh, S.N., Mohammadi, F., 2008. Development of an artificial neural network model for prediction of cell voltage and current efficiency in a chlor-alkali membrane cell. Chem. Eng. Res. Des. 86, 461–472. https://doi.org/10.1016/j.cherd.2007.12.009.
Strathmann, H., Krol, J.J., Rapp, H.-J., Eigenberger, G., 1997. Limiting current density and water dissociation in bipolar membranes. J. Memb. Sci. 125, 123–142. https://doi.org/10.1016/S0376-7388(96)00185-8.
Strathmann, H., 2004. Ion-Exchange Membrane Separation Processes, First edit. Elsevier B.V.
Trivedi, G.S., Shah, B.G., Adhikary, S.K., Indusekhar, V.K., Rangarajan, R., 1997. Studies on bipolar membranes. Part II - conversion of sodium acetate to acetic acid and sodium hydroxide. React. Funct. Polym. 32, 209–215. https://doi.org/10.1016/S1381-5148(96)00088-0.
Uwuigbe, U., Issah, O., Ranti, U.O., Zubeiru, M., Anaba, S., Seidu, A.A.J., 2025. Circular Economy: a bibliometric review of research in emerging economies (2010-2024). Int. J. Energy Econ. Policy 15, 77–89. https://doi.org/10.32479/ijeep.17021.
Vallès, V., Fernández de Labastida, M., López, J., Battaglia, G., Winter, D., Randazzo, S., Cipollina, A., Cortina, J.L., 2023. Sustainable recovery of critical elements from seawater saltworks bitterns by integration of high selective sorbents and reactive precipitation and crystallisation: developing the probe of concept with on-site produced chemicals and energy. Sep. Purif. Technol. 306. https://doi.org/10.1016/j.seppur.2022.122622.
Vassallo, F., La Corte, D., Cancilla, N., Tamburini, A., Bevacqua, M., Cipollina, A., Micale, G., 2021. A pilot-plant for the selective recovery of magnesium and calcium from waste brines. Desalination 517. https://doi.org/10.1016/j.desal.2021.115231.
Virruso, G., Cassaro, C., Tamburini, A., Cipollina, A., Micale, G.D.M., 2023. Performance evaluation of an electrodialysis with bipolar membranes pilot plant operated in feed & bleed mode. Chem. Eng. Trans. 105, 73–78. https://doi.org/10.3303/CET23105013.
G. Virruso, C. Cassaro, W.M. Ashraf, A. Tamburini, V. Dua, I.D.L. Bogle, A. Cipollina, G. Micale, Dynamic modelling of electrodialysis with bipolar membranes using NARX recurrent neural networks, 2024a. https://doi.org/10.1016/B978-0-443-28824-1.50031-4.
Virruso, G., Cassaro, C., Culcasi, A., Cipollina, A., Tamburini, A., Bogle, I.D.L., Micale, G D.M., 2024b. Multi-scale modelling of an electrodialysis with bipolar membranes pilot plant and economic evaluation of its potential. Desalination. 583, 117724. https://doi.org/10.1016/j.desal.2024.117724.
Virruso, G., Cassaro, C., Vassallo, F., Filingeri, A., Pellegrino, A., Tamburini, A., Cipollina, A., Micale, G.D.M., 2025a. A pilot plant investigation on a real seawater brine valorisation via electrodialysis with bipolar membranes. J. Water Process Eng. 69, 106741. https://doi.org/10.1016/J.JWPE.2024.106741.
Virruso, G., Cassaro, C., Cipollina, A., Tamburini, A., Micale, G., 2025b. Novel approaches for valorisation of waste brines at pilot scale via electrodialysis with bipolar membranes. Desalination.
Ye, Z., Yin, X., Chen, L., He, X., Lin, Z., Liu, C., Ning, S., Wang, X., Wei, Y., 2019. An integrated process for removal and recovery of Cr(VI) from electroplating wastewater by ion exchange and reduction–precipitation based on a silica-supported pyridine resin. J. Clean. Prod. 236. https://doi.org/10.1016/j.jclepro.2019.117631.